

The effect of lightweight aggregate on drying shrinkage and properties of one-part alkali activated slag concrete

Razieh Kadkhodaei (✉ kadkhodai7290@gmail.com)

Isfahan University of Technology

Kiachehr Behfarnia

Isfahan University of Technology

Marjan Shahidi

Isfahan University of Technology

Research Article

Keywords: Lightweight concrete, One-part alkali-activated slag, Sodium metasilicate, Drying shrinkage, Curing

Posted Date: May 11th, 2022

DOI: <https://doi.org/10.21203/rs.3.rs-1611047/v1>

License:  This work is licensed under a Creative Commons Attribution 4.0 International License.

[Read Full License](#)

Abstract

In the present study, the result of slag grade, dosage of activator and aggregate combination on the compressive strength and drying shrinkage of one-part alkali-activated slag concrete was considered. Also, water curing and plastic cover curing were selected to investigate the effect of curing condition on drying shrinkage and compressive strength of this type of concrete. Two aggregate combinations, one containing lightweight fine (LAF) and normal weight coarse (NAC) aggregates and one other containing both lightweight fine and coarse aggregates, were considered for making the lightweight concrete and conducting the experimental tests. Compressive strength of the specimens were measured at 7, 28 and 90 days, as well as drying shrinkage strain up to 180 days. According to the results, in most of the mixtures, slump and setting time decreased with increasing slag and activator content, while compressive strength and drying shrinkage increased. Examination of curing condition of one-part lightweight alkali-activated slag concrete showed that drying shrinkage increased and compressive strength decreased with plastic cover curing at later age.

1. Introduction

Concrete is a common and the most critical material used in construction. Increasing the usage of concrete and the need for cement manufacturing, and the vital role of environmental matters and particular emphasize on sustainability of improvement have led into requirement for reviewing production of cement to become clear (H. A. Abdel-Gawwad, Mohammed, & Alomayri, 2019). Employing industrial side products as the binder is a good example of possible selection instead of the Ordinary Portland cement. This cementitious material has low environmental impact, and better performance such as high mechanical properties (Behfarnia & Rostami, 2017; R. J. Thomas, Gebregziabiher, Giffin, & Peethamparan, 2018), high acid resistance (Sturm, Gluth, Jäger, Brouwers, & Kühne, 2018; Temuujin, Minjigmaa, Lee, Chen-Tan, & van Riessen, 2011), fire (H. Y. Zhang, Kodur, Qi, Cao, & Wu, 2014), freeze and thaw (Shahrajabian & Behfarnia, 2018) and abrasion (Mohebi, Behfarnia, & Shojaei, 2015) than Ordinary Portland cement, thereby being able to be used as a part or 100 substituted material with cement in preparing concrete and evolving as the most reassuring cementitious material taking the place of cement (Cheng et al., 2018). The employment of binders which are alkali-activated on the basis of materials high in calcium, has received a lot of attention, by bringing into play the granulated ground blast furnace slag and other industrial by-products (Pacheco-Torgal, Labrincha, Leonelli, Palomo, & Chindaprasit, 2014). Conventional (two-part) alkali-activated binders are constructed by a reaction happened between a solution of alkali hydroxide, silicate, carbonate, or sulfate which is aqueously concentrated for example, and solid aluminosilicate precursor which is two parts supplying to water (Duxson, Fernández-Jiménez, et al., 2007; Provis, 2009, 2014; Provis & Van Deventer, 2013). Nevertheless, there are some impracticalities associated with dealing with the huge quantities of viscous, corrosive, and perilous alkali-activator solutions have applied a lot of pressure to the development of one-part alkali-activated binders. That could be used similarly to ordinary Portland cement (Luukkonen, Abdollahnejad, Yliniemi, Kinnunen, & Illikainen, 2018). To solve the problems caused by two-part alkali-activated binders, one-part alkali-

activated binders were prepared by mixing a precursor of solid aluminosilicate, a solid alkaline material, and practicable additives in composition to water. However CO₂ emission is possible to be reduced by 25–50% (Duxson, Provis, Lukey, & van Deventer, 2007; Robert J Thomas, Ye, Radlinska, & Peethamparan, 2016), using materials which are alkali-activated, but they have not gained consideration from the industry as a result of the long-term properties they perform, especially drying shrinkage. The most crucial reason which narrows the extended application of this material is the micro –cracks which root in drying shrinkage (Melo Neto, Cincotto, & Repette, 2008; Ye & Radlińska, 2016). The drying shrinkage of alkali-activated concrete is under the influence of raw materials reaction, dose and type of chemical activator and condition of curing (Melo Neto et al., 2008).

It is illustrated by Collins and Sanjayan that the drying shrinkage of alkali-activated slag is approximately three times bigger than it is in OPC concrete provided for specimens which are cured at the surrounding temperature of 23 °C and the relative humidity of 50% (Collins & Sanjayan, 2000). The chemical features of the activator is able to have a determinant impact on the shrinkage of alkali-activated slag. Behfarnia and Rostami shown the direct relationship between the properties of alkali-activated slag concrete and the ratio of alkali to slag (Behfarnia & Rostami, 2018). Taghvaei et al. investigated the influences of sodium silicate modulus and concentration of alkali on the properties of alkali-activated slag concrete. They reported an optimum concentration of 5.5% and a silicate modulus of 0.85 in order to avoid rapid setting time, reduced high drying shrinkage and compressive strength (Taghvayi, Behfarnia, & Khalili, 2018). Neto et al. carried out a study on how different activators affect drying and autogenous shrinkages of AAS in a way in which a silica modulus of 1.7 (SiO₂/ Na₂O) had activated the slag binders and the slag mass was 2.5, 3.5 and 4.5% Na₂O. The results showed an increase in the total shrinkage (drying and autogenous) by increasing the amount of SiO₂ and Na₂O in a manner in which the drying shrinkage was considerable in comparison with the autogenous shrinkage (Melo Neto et al., 2008). In addition to activator, drying shrinkage and the properties of the alkali-activated slag concrete are also affected by the curing conditions including temperature and relative humidity (Komljenović, Bašcarević, & Bradić, 2010; Pacheco-Torgal et al., 2014). Mohebi et al. mentioned that compressive strength was increased with temperature curing. The kinetic energy was increased by heat curing and also the development of strength was accelerated. Also, at high temperatures (60–95 °C) the development rate of compressive strength was lessened (Mohebi et al., 2015). The time of temperature curing has a great effect on strength. Too much time of temperature curing can reduce performance of alkali-activated concrete (Singh, Ishwarya, Gupta, & Bhattacharyya, 2015). The results of Kumarawal's experiments shows that the compressive strength of the specimens cured in oven is higher than environmental curing and the optimum compressive strength was obtained at 60 ° C (Kumaravel, 2014).

Table 1
The chemical composition of the materials (%)

Material	SiO ₂	Al ₂ O ₃	Fe ₂ O ₃	CaO	MgO	SO ₃	K ₂ O	Na ₂ O	L.O.I
Slag	36.50	11.00	1.00	38.50	7.80	0.30	0.80	0.65	n.a.
Cement	32.50	5.80	3.10	60.00	3.10	2.00	n.a.	n.a.	1.10

Table 2
The chemical composition of the sodium metasilicate.5H₂O (%)

SiO ₂	Na ₂ O	H ₂ O
29.50 ± 0.2	29.50 ± 0.2	41

Table 3
properties of lightweight fine aggregate

Apparent density (kg/m ³)	Bulk density (kg/m ³)	Water absorption (%)	Fineness modulus
1400	800	10	2.45

Table 4
properties of lightweight coarse aggregate

Apparent density (kg/m ³)	Bulk density (kg/m ³)	Water absorption (%)	Diameter (mm)
1300	700	8	< 12.5

Table 5
Mix composition

Mix	Slag (kg/m ³)	Sodium metasilicate (kg/m ³)	Added water (kg/m ³)	Fine Aggregate		Coarse aggregate		Type of curing
				LAF	NAF	LAC	NAC	
A1	400	72	156.32	498.94	-	308.8	-	Water
A2	475	85.5	185.6	439.7	-	272.2	-	Water
A3	400	80	155	492.9	-	305.2	-	Water
A4	400	72	156.32	498.94	-	308.8	-	Plastic cover
A5	475	95	184.1	432.6	-	267.8	-	Water
A6	475	95	184.1	432.6	-	-	545.9	Water
A7	475	95	184.1	-	834.4	-	545.9	Water
OPC	C = 442.48, w/c = 0.42		185.84	484.6	-	323.1	-	Water

Findings show that drying shrinkage of alkali-activated slags can be reduced by heat curing. It can be due to the limited unbound water consumption during chemical reactions. Unbound water lose over time can result in notable drying shrinkage strains for alkali-activated binders that cured at ambient temperature, particularly within the first two weeks (Chi & Huang, 2013; Wallah & Rangan, 2006). Zijian et al. investigated the effect of relative humidity on the shrinkage by using expanders. The results showed that the shrinkage in the alkali-activated slag mortar is linearly correlated with the relative humidity (Jia, Yang, Yang, Zhang, & Sun, 2018) and in addition, the time of curing, the difference between ambient temperature and concrete, effect on the rate of evaporation water from the concrete surface and consequently the shrinkage (Hasanain, Khallaf, & Mahmood, 1989). However, drying shrinkage is dependent on binder, the amount and type of aggregate is affected in limiting the drying shrinkage. Light weight composites have extent absorbency and before being mixed are prewetted to make sure there is no water lose from the mixture. After the concrete is set, the stores water in the composites releases gradually, this makes cementitious materials able to keep hydration after the termination of the external curing, as long as the composites contain water. The difference between the additional water absorbed in aggregates influences the amplitude of drying shrinkage in concrete with light weight or normal weight during the stage of hardening in which significant changes take place in the properties of the concrete over time, especially in comparatively first stages. As the light weight coarse composites absorbency is significantly higher than in composites with normal weight, the result of water excess is reducing the light weight concrete during shrinkage (Jiajun, Shuguang, Fazhou, Yufei, & Zhichao, 2006). Meg and Khayat's findings illustrate that using light weight sand in UHPC containing 4% silica fume, 34% class C fly ash with 0.2 w/b is able to decrease the relative humidity and autogenous shrinkage considerably. Absence of light weight sand and presence of 75% light weight sand showed relative humidity of roughly 83% and

93%, respectively at 7 days. Before being mixed and used for internal curing, light weight aggregate is a good candidate to be saturated for the aim of water accumulation (Meng & Khayat, 2017). Then the accumulated water release in the period of hydration of binders into the system in order to make up for the loss of moisture and decrease shrinkage. Existing studies have shown different results on the shrinkage of lightweight aggregate. Light-weight concrete in comparison with normal weight aggregate concrete showed smaller shrinkage in ref (Fujiwara, 2008; LIN, 2004; Lura, Van Breugel, & Maruyama, 2002), while in contrast the shrinkage in ref (Al-Attar, 2008; Asamoto, Ishida, & Maekawa, 2008; M. H. Zhang, Li, & Paramasivam, 2005) was more. The reason can be the variety of moisture load corresponding light-weight concrete drying shrinkage during the time differing highly with those of normal weight concrete, especially in the stage of hardening (Fujiwara, 2008). In this research the effect of slag content in one-part lightweight alkali-activated slag concrete (OLWAAS) mixture that activated with sodium metasilicate with weight ratio of 18% and 20% of slag and two curing methods, such as water curing and plastic cover curing on the slump, setting time, compressive strength and drying shrinkage were studied and examined. To investigation the effect of lightweight aggregate on properties and drying shrinkage of OLWAAS, replacement fine aggregate, coarse and both with Leca as lightweight aggregate, respectively.

2. Material

In this study, the slag of Sepahan cement factory with a density of 2.780 was used. For activation of the slag, a solid powder of sodium metasilicate.5H₂O with a chemical formula (Na₂SiO₃.5H₂O) of Silica Gostar product with a mass of 950 g / L and a molar ratio of 1 was used. The binder materials include slag and dry part of sodium metasilicate for made OLWAAS and Portland cement type I from Sepahan cement factory for made lightweight Portland cement concrete (OPC). The chemical composition of cement, sodium metasilicate and slag are illustrated in Table 1 and

Table 2. The slag contents in the concrete were 400 and 475 kg/m³ and the weight ratios of one-part alkali activator to the slag were 18% and 20%. Fine aggregate (river sand) was used with fineness modulus of 3.1 and saturated surface dry specific gravity of 2.7, and crushed stone (coarse aggregate) which the maximum normal size is 12.5 mm and the specific gravity of the saturated surface is 2.65 were also used in this study. The properties of fine and coarse light weight aggregates are shown in Table 3 and 4.

3. Mix Design, Preparation And Samples Curing

To make lightweight concrete and investigate the effect of the lightweight aggregate in volume replacement on the compressive strength and drying shrinkage, four mixes were designed. In this study, the lightweight aggregates were soaked in water for 24 h before mixing and used as the pre-wetted lightweight aggregate. Two aggregate combinations, one containing lightweight fine (LAF) and normal weight coarse (NAC) aggregates and one other containing both lightweight fine and coarse aggregates, were considered for making the lightweight concrete and conducting the experimental tests. A7 mix

(containing normal weight aggregates) was designed to be compared with the lightweight ones. Portland cement specimen (OPC mix) was also made to control and compare the slag with cement. The cement content in the OPC mix ($C = 442.48 \text{ kg/m}^3$) was equal to the binder content of A5, A6 and A7 mixes. The volume of fine and coarse aggregates in A5, A6 and A7 mixes was constant. Specimen proportion of the mixture in this experiment is illustrated in Table 5. The water to binder ratio in all of the mixtures was 0.42 to ensure its workability. Binder content in A1 to A7 mixes consisted of slag content and the solid part of sodium metasilicate. The sum of the existing water in sodium metasilicate and water added to the mixture represented the amount of water the experiment used. The compressive strength values were measured according to BS 1881 (BS, 1983). Specimen's casting was done in a mold with the size of $100 \times 100 \times 100 \text{ mm}$ and curing was done in a standard curing room ($23 \pm 2^\circ\text{C}$) for 48 h. After demolding, the specimens were cured in water or plastic cover until the time of experiment. Figure 1 shows how the samples were cured. The dimensions of the prismatic specimen used to measure the drying shrinkage were $75 \times 75 \times 285$. In this research, 3 prism samples were applied in each mixture to measure the sample length variation. As illustrated in Fig. 2, the specimen strain measurements were implemented by using the DEMEC strain gauge having fixed points on the specimen's both sides with the 8 micro strain accuracy.

4. Test Procedure, Result And Discussion

4.1. Slump

The slump test was carried out according to ASTM C143 (ASTM, 2012). The results of the slump test for mixes are shown in Fig. 3. According to Fig. 3a, the slump was decreased when the slag content was increased. Increasing the slag content from 400 to 475 kg/m^3 decreased the slump by 14%.

With regard to Fig. 3a, the slump was decreased with increasing the sodium metasilicate (one-part alkali-activator). By increasing the sodium metasilicate ratio from 18 to 20%, the slump was decreased by 18–20%. Behfarnia and Rostami have reported similar results when using sodium hydroxide and sodium silicate for the activation of the slag (Behfarnia & Rostami, 2018). At a constant water/ binder ratio (here 0.42), with increasing the one-part alkali activator, the volume of the added water was decreased; also, its chemical reactions could be accelerated and intensified, leading to the reduction of the slump. Thus, it seems that with increasing the alkali activator, the measured slump of the alkali-activated slag concrete was decreased. Figure 3b shows the effect of the aggregate combination on the measured slump in the mixes with the slag content of 475 kg/m^3 and the sodium metasilicate ratio of 20%. According to Fig. 3b, the maximum slump was observed in the A7 mix, which was about 110 mm. As can be seen from Fig. 3b, the other mixes containing the lightweight aggregate (Leca) had less slump in comparison to the normal weight aggregate ones. According to the results brought in Fig. 3b, the measured slump was 78 and 64 mm in A5 and A6 mixes, which was about 21% and 23% lower than that for the A7 mix, respectively.

4.2. Setting time

The test was carried out in accordance with ASTM C191 (ASTM, 2008). The results of the initial and final setting times are illustrated in Fig. 4. So, setting time was affected by the type and dosage of the used alkali-activator. According to Fig. 4, increasing the sodium metasilicate (one-part alkali activator) decreased the initial and final setting times. With increasing the sodium metasilicate from 18% (A1) up to 20% (A3), the initial setting time was decreased from 90 to 73 min; the final setting time was also reduced about 11%. In the one-part geopolymer, the initial and final setting times were in the range of 23–150 and 69–230 minutes, respectively (H. Abdel-Gawwad & Abo-El-Enein, 2016; Matalakah, Xu, Wu, & Soroushian, 2017; Wang, Du, Lv, He, & Cui, 2017). Yang et al. also found out that using the solid activator instead of the solution activator caused the alkali activated blast furnace slag to be hardened more slowly (Yang, Song, Ashour, & Lee, 2008).

4.3. Compressive strength

The compressive strength test was measured on the specimens according to BS 1881 (1881, 1983) upon 7, 28 and 90 days. The effects of the slag content, the percentage of sodium metasilicate, aggregate composition and the type of curing on the compressive strength are shown in Figs. 5 to 7.

At first, by comparing the compressive strength of OPC and one-part lightweight alkali-activated (OLWAAS) concrete, as shown in Fig. 5, one-part lightweight alkali-activated slag concrete gained more strength than the lightweight Portland cement one. These results also showed that OLWAAS generally possessed a higher strength gain rate, as compared to the OPC concrete, as a result of the higher rate of the C-A-S-H formation of the gel when the slag was activated with sodium metasilicate (one-part alkali-activator). The results also showed that strength development was 87% and 75% in the OLWAAS concrete from 7 days to 28 and 90days, respectively; also, the strength development was 70% in the OPC concrete from 7 to 28-days. According to the results brought in Fig. 5, the compressive strength of the A1 concrete was about 60, 30 and 20% higher than that of the OPC concrete upon 7, 28 and 90 days, respectively.

In the following, the effect of each parameter on the compressive strength of the OLWAAS concrete is addressed.

Figure 6a shows the effect of slag content on the compressive strength at a constant sodium metasilicate ratio of 18% and water curing. Increasing slag content from 400 to 475 kg/m³, increased the compressive strength about 10.1, 10.5 and 9% at 7, 28 and 90-day, respectively. To explain this observation, it can be argued that enough slag content in the mixture at low water/binder ratio, make the binder denser and improved compressive strength. The presence of calcium assists the setting and hardening with the development of C-S-H and with continuing alkali-slag reaction, the increase of C-S-H gel filled the pores of the geopolymer matrix. The filling effect and alkali-slag reactions are also beneficial for improving the microstructure and compressive strength.

The effects of water and plastic cover curing on the compressive strength of the OLWAAS concrete, the mixes A1 and A4, were measured upon 7, 28 and 90days, as plotted in Fig. 6c. These results also certified that by curing in water and plastic cover, the compressive strength trend was increased at all ages.

Throughout the experiments, it was observed that the compressive strength of the samples subjected to plastic cover curing had a better performance at an early age, as compared to water curing. The compressive strength of the samples with the slag content of 400 kg/m^3 and sodium metasilicate ratio of 18%, when cured in plastic cover, was 4.4 and 3% higher than that done in water upon 7 and 28 days. However, at the later age, despite the increasing trend, the compressive strength of the sample cured in the plastic cover was 6.7% lower, as compared to water curing upon 90 days. This can be explained by the fact that, at an older age, the OLWAAS concrete was trapped in plastic cover, so it had lower water to continue the slag reaction, in comparison to water curing at the same age.

Figure 7 shows the effect of the aggregate combination on the compressive strength upon 7, 28 and 90 days. As expected, the highest compressive strength was observed in the A7 mixture at all ages and the other mixes including A6 and A5 gained less. With regard to Fig. 7, the compressive strength of A6 and A5 mixtures was about 57 and 46% lower than that of the FC mix upon 28 days, respectively.

4.4. Drying shrinkage

The drying shrinkage test was measured on the samples up to 180 days after curing, according to ASTM C157 (ASTM, 2014). At first, by comparing the drying shrinkage of OLWAAS and OPC concrete types, as shown in Fig. 8, the drying shrinkage was 1.8 times more than that of the OPC concrete. The drying shrinkage of the OLWAAS concrete, A1 mixture, was measured to be 1004 micro strain after 180 days, while for the OPC concrete, this was 554, this could be due to unbound water partial consumption toward chemical reactions in OLWAAS.

Figure 9a shows the effect of the slag content on the drying shrinkage of the sample with sodium metasilicate ratio of 18% and water curing. As shown Fig. 9a, with increasing the slag content, the drying shrinkage was improved. With increasing the slag content from 400 to 475 kg/m^3 , the ultimate drying shrinkage was increased about 10% in the A2 mixture. The drying shrinkage was highly dependent on the binder. Therefore, with increasing the volume of the binder, the concrete was more prone to it. As the slag content was raised, at the constant water/binder ratio, the added water was increased in the concrete mix and the volume of aggregate was decreased, so there was more water to evaporate from concrete, causing more drying shrinkage. Figure 9b presents the drying shrinkage test results of the OLWAAS concrete with the slag content of 400 kg/m^3 and water curing for different percents of the activator. 18% and 20% sodium metasilicate resulted in 1004 and 1080 microstrain for the drying shrinkage, respectively. As the activator was increased, the alkali-slag reaction and gel production were enhanced; the free water in the silicate gel was raised as well. As a result, after placing samples for drying, the drying shrinkage of the samples was improved with increasing the one-part alkali-activator (sodium metasilicate).

The drying shrinkage of the one-part alkali-activated concrete was affected by the type of curing. In this research, two types of curing (water and plastic cover curing) were examined. Figure 9c shows that the drying shrinkage of the samples cured in plastic cover (A4 mix) was about 1097 and 1004 micro strain for the samples cured in water (A1 mix). With curing the OLWAAS concrete in water, the binder absorbed

water from the curing ambient to continue the alkali-slag reaction during the curing period. Absorbency of lightweight aggregates was high and they were prewetted prior to being mixed. The stored water in the aggregates was released gradually over time after the concrete had been set, letting the binder to continue the alkali-slag reaction after the termination of the external curing as long as aggregates contained water. At the same time, the concrete trapped in plastic cover used the water that had been stored by lightweight aggregate to continue the alkali-slag reaction; so, after the curing period, it had less water than the one cured in water. Figure 10 shows the drying shrinkage of the one-part alkali activated slag concrete with different aggregate combinations. The drying shrinkage in the light weight concrete was higher than that of the normal weight aggregate concrete; however, pre-wetting lightweight aggregates and internal curing could be carried out to decrease the drying shrinkage in the lightweight concrete. As the concrete hardening progressed and the effect of internal curing was diminished, as compared to the normal weight concrete, the lightweight concrete resulted in the lower drying shrinkage, as compared to that of the normal one. The water stored in pre-wetting the lightweight aggregate maintained the saturation of the binder, thereby decreasing the drying shrinkage. According to the results, the drying shrinkage of the mix without Leca was 1520 micro strain, so it was lower than that in the lightweight mixes upon 180 days.

5. Sem

This study used images obtained by SEM for the comparison of the microstructures belonging to the AAS pastes that had been cast with various combinations of aggregates. These images were developed for some samples including A5, A6 and A7 which were in the age of 180 days. The conditions related to curing, slag content and the dosage of the samples activator were like those of the drying shrinkage. In the case of mixes having a denser microstructure, as could be seen on the basis of the SEM image shown in **Fig. 11**, the drying shrinkage showed reduction. As can be seen in **Figs. 11b and 11c**, in regard to the mixtures which contained the lightweight aggregates, the densification of AAS paste microstructures occurred and there was the reduction of the free space existing between the hydration products. In the case of the conventional concrete, a larger replacement level for lightweight aggregates in the mixtures was observed; this considerably decreased the drying shrinkage; on the other hand, the low contents of replacement was not effective on the mitigation of the drying shrinkage that had been due to external drying (Henkensiefken, Bentz, Nantung, & Weiss, 2009). Water existing in the pre-wetted lightweight aggregate could keep the paste saturation, thereby reducing the drying shrinkage. Due to the lightweight aggregate larger pore size, in comparison to those related to the hydrating paste, water was moved from the lightweight aggregate to the paste surrounding it (albeit larger pores), producing the lower capillary stress, which led to the reduction of the drying shrinkage as well as the cracking tendency.

As can be seen in Fig. 11c, in the case of the A7 mix, with a hydration products microstructure, a small number of void spaces were developed, in comparison to the A5 and A6 ones; as can be seen in Fig. 11a and 11b, based on the results brought in section 4.4 (Fig. 10), application of fine and coarse lightweight aggregates in the mixture led to the lower drying shrinkage. Adding LWA enhanced the driving force for water; as a result, a higher amount water was devoted to the hydration at the later ages. The hydration

increase could decrease the porosity and make improvement in the antipermeability, thereby decreasing the drying shrinkage.

6. Conclusion

In this study, the effect of different parameters on the compressive strength and drying shrinkage of the one-part alkali activated slag (OLWAAS) concrete was investigated. The results of this study can be summarized here:

1. As the slag content was increased from 400 to 475 kg/m³, the slump was decreased, while the compressive strength and drying shrinkage in the OLWAAS concrete were increased.
2. A 10% increase in the one-part activator for the OLWAAS concrete reduced slump by 16%, as well as decreasing the initial and final setting times. But raising this parameter, the compressive strength was increased at all ages; the drying shrinkage was improved as well.
3. Plastic cover curing of the OLWAAS concrete had a better performance in terms of compressive strength at an early age in comparison to water. However, at the later age, the samples cured in the plastic cover showed a compressive strength lower than that obtained in water, which was by 7%. Regarding the effect of the type of curing on the drying shrinkage, the results showed that the OLWAAS concrete cured in the plastic cover had a greater drying shrinkage in comparison to a similar sample cured in water.
4. Regarding the mixes containing lightweight aggregates, A5 and A6, to make lightweight concrete, they had the lowest compressive strength and drying shrinkage, as compared to the A7 mix. The Pre-wetting lightweight aggregate decreased the drying shrinkage.
5. The rate of the gain compressive strength at an early age in the OLWAAS concrete was higher than that in the OPC concrete and 87% of its 28-day compressive strength was achieved in the first 7 days. Examination of the drying shrinkage results also showed that the drying shrinkage of the OLWAAS concrete was about 1.8 times higher than that of the OPC sample.

References

1. , B. (1983). Testing concrete. Method for determination of compressive strength of concrete cubes 116 (pp. 10). London: British Standard Institution.
2. Abdel-Gawwad, H., & Abo-El-Enein, S. (2016). A novel method to produce dry geopolymer cement powder. *HBRC journal*, 12(1), 13-24.
3. Abdel-Gawwad, H. A., Mohammed, M. S., & Alomayri, T. (2019). Single and dual effects of magnesia and alumina nano-particles on strength and drying shrinkage of alkali activated slag. *Construction and Building Materials*, 228, 116827. doi:<https://doi.org/10.1016/j.conbuildmat.2019.116827>

4. Al-Attar, T. S. (2008). Effect of coarse aggregate characteristics on drying shrinkage of concrete. *Engineering and Technology Journal*, 26(2), 146-153.
5. Asamoto, S., Ishida, T., & Maekawa, K. (2008). Investigations into Volumetric Stability of Aggregates and Shrinkage of Concrete as a Composite. *Journal of Advanced Concrete Technology*, 6(1), 77-90. doi:10.3151/jact.6.77
6. ASTM. (2008). C191-82 , Standard Test Methods for Time of Setting of Hydraulic Cement by Vicat Needle. USA: *ASTM International*.
7. ASTM. (2012). C143/C143M-12-Standard Test Method for Slump of Hydraulic-Cement Concrete. USA: *ASTM International*.
8. ASTM. (2014). C157, Standard Test Method for Length Change of Hardened Hydraulic-Cement Mortar and Concrete. USA: *ASTM International*.
9. Behfarnia, K., & Rostami, M. (2017). Mechanical Properties and Durability of Fiber Reinforced Alkali Activated Slag Concrete. *Journal of materials in civil engineering*, 29(12), 04017231. doi:doi:10.1061/(ASCE)MT.1943-5533.0002073
10. Behfarnia, K., & Rostami, M. (2018). The Effect of Alkaline Solution-to-Slag Ratio on Permeability of Alkali Activated Slag Concrete. *International Journal of Civil Engineering*, 16(8), 897-904. doi:10.1007/s40999-017-0234-3
11. BS. (1983). 1881, Testing concrete. Method for determination of compressive strength of concrete cubes. *British Standard Institution*.
12. Cheng, Y., Hongqiang, M., Hongyu, C., Jiabin, W., Jing, S., Zonghui, L., & Mingkai, Y. (2018). Preparation and characterization of coal gangue geopolymers. *Construction and Building Materials*, 187, 318-326. doi:https://doi.org/10.1016/j.conbuildmat.2018.07.220
13. Chi, M., & Huang, R. (2013). Binding mechanism and properties of alkali-activated fly ash/slag mortars. *Construction and Building Materials*, 40, 291-298. doi:https://doi.org/10.1016/j.conbuildmat.2012.11.003
14. Collins, F., & Sanjayan, J. G. (2000). Effect of pore size distribution on drying shrinking of alkali-activated slag concrete. *Cement and Concrete Research*, 30(9), 1401-1406. doi:https://doi.org/10.1016/S0008-8846(00)00327-6
15. Duxson, P., Fernández-Jiménez, A., Provis, J. L., Lukey, G. C., Palomo, A., & van Deventer, J. S. (2007). Geopolymer technology: the current state of the art. *Journal of materials science*, 42(9), 2917-2933.
16. Duxson, P., Provis, J. L., Lukey, G. C., & van Deventer, J. S. J. (2007). The role of inorganic polymer technology in the development of 'green concrete'. *Cement and Concrete Research*, 37(12), 1590-1597. doi:https://doi.org/10.1016/j.cemconres.2007.08.018
17. Fujiwara, T. (2008). Effect of Aggregate on Drying Shrinkage of Concrete. *Journal of Advanced Concrete Technology*, 6(1), 31-44. doi:10.3151/jact.6.31
18. Hasanain, G. S., Khallaf, T. A., & Mahmood, K. (1989). Water evaporation from freshly placed concrete surfaces in hot weather. *Cement and Concrete Research*, 19(3), 465-475. doi:https://doi.org/10.1016/0008-8846(89)90035-5

19. Henkensiefken, R., Bentz, D., Nantung, T., & Weiss, J. (2009). Volume change and cracking in internally cured mixtures made with saturated lightweight aggregate under sealed and unsealed conditions. *Cement and Concrete Composites*, 31(7), 427-437.
doi:<https://doi.org/10.1016/j.cemconcomp.2009.04.003>
20. Jia, Z., Yang, Y., Yang, L., Zhang, Y., & Sun, Z. (2018). Hydration products, internal relative humidity and drying shrinkage of alkali activated slag mortar with expansion agents. *Construction and Building Materials*, 158, 198-207. doi:<https://doi.org/10.1016/j.conbuildmat.2017.09.162>
21. Jiajun, Y., Shuguang, H., Fazhou, W., Yufei, Z., & Zhichao, L. (2006). Effect of pre-wetted light-weight aggregate on internal relative humidity and autogenous shrinkage of concrete. *Journal of Wuhan University of Technology-Mater. Sci. Ed.*, 21(1), 134-137. doi:10.1007/bf02861491
22. Komljenović, M., Baščarević, Z., & Bradić, V. (2010). Mechanical and microstructural properties of alkali-activated fly ash geopolymers. *Journal of Hazardous Materials*, 181(1), 35-42.
doi:<https://doi.org/10.1016/j.jhazmat.2010.04.064>
23. Kumaravel, S. (2014). Development of various curing effect of nominal strength Geopolymer concrete. *Journal of Engineering Science and Technology Review*, 7(1), 116-119.
24. LIN, S. (2004). *Early age deformation characteristics of high performance concrete*.
25. Lura, P., Van Breugel, K., & Maruyama, I. (2002). Autogenous and drying shrinkage of high-strength lightweight aggregate concrete at early ages– The effect of specimen size. *PRO*, 23, 335-342.
26. Luukkonen, T., Abdollahnejad, Z., Yliniemi, J., Kinnunen, P., & Illikainen, M. (2018). One-part alkali-activated materials: A review. *Cement and Concrete Research*, 103, 21-34.
doi:<https://doi.org/10.1016/j.cemconres.2017.10.001>
27. Matalkah, F., Xu, L., Wu, W., & Soroushian, P. (2017). Mechanochemical synthesis of one-part alkali aluminosilicate hydraulic cement. *Materials and Structures*, 50(1), 97.
28. Melo Neto, A. A., Cincotto, M. A., & Repette, W. (2008). Drying and autogenous shrinkage of pastes and mortars with activated slag cement. *Cement and Concrete Research*, 38(4), 565-574.
doi:<https://doi.org/10.1016/j.cemconres.2007.11.002>
29. Meng, W., & Khayat, K. (2017). Effects of saturated lightweight sand content on key characteristics of ultra-high-performance concrete. *Cement and Concrete Research*, 101, 46-54.
30. Mohebi, R., Behfarnia, K., & Shojaei, M. (2015). Abrasion resistance of alkali-activated slag concrete designed by Taguchi method. *Construction and Building Materials*, 98, 792-798.
doi:<https://doi.org/10.1016/j.conbuildmat.2015.08.128>
31. Pacheco-Torgal, F., Labrincha, J., Leonelli, C., Palomo, A., & Chindaprasit, P. (2014). *Handbook of alkali-activated cements, mortars and concretes*. Elsevier.
32. Provis, J. L. (2009). Activating solution chemistry for geopolymers *Geopolymers* (pp. 50-71): Elsevier.
33. Provis, J. L. (2014). Geopolymers and other alkali activated materials: why, how, and what? *Materials and Structures*, 47(1-2), 11-25.

34. Provis, J. L., & Van Deventer, J. S. (2013). *Alkali activated materials: state-of-the-art report, RILEM TC 224-AAM* (Vol. 13): Springer Science & Business Media.
35. Shahrajabian, F., & Behfarnia, K. (2018). The effects of nano particles on freeze and thaw resistance of alkali-activated slag concrete. *Construction and Building Materials, 176*, 172-178. doi:<https://doi.org/10.1016/j.conbuildmat.2018.05.033>
36. Singh, B., Ishwarya, G., Gupta, M., & Bhattacharyya, S. K. (2015). Geopolymer concrete: A review of some recent developments. *Construction and Building Materials, 85*, 78-90. doi:<https://doi.org/10.1016/j.conbuildmat.2015.03.036>
37. Sturm, P., Gluth, G. J. G., Jäger, C., Brouwers, H. J. H., & Kühne, H. C. (2018). Sulfuric acid resistance of one-part alkali-activated mortars. *Cement and Concrete Research, 109*, 54-63. doi:<https://doi.org/10.1016/j.cemconres.2018.04.009>
38. Taghvayi, H., Behfarnia, K., & Khalili, M. (2018). The Effect of Alkali Concentration and Sodium Silicate Modulus on the Properties of Alkali-Activated Slag Concrete. *Journal of Advanced Concrete Technology, 16*(7), 293-305.
39. Temuujin, J., Minjigmaa, A., Lee, M., Chen-Tan, N., & van Riessen, A. (2011). Characterisation of class F fly ash geopolymer pastes immersed in acid and alkaline solutions. *Cement and Concrete Composites, 33*(10), 1086-1091. doi:<https://doi.org/10.1016/j.cemconcomp.2011.08.008>
40. Thomas, R. J., Gebregziabiher, B. S., Giffin, A., & Peethamparan, S. (2018). Micromechanical properties of alkali-activated slag cement binders. *Cement and Concrete Composites, 90*, 241-256. doi:<https://doi.org/10.1016/j.cemconcomp.2018.04.003>
41. Thomas, R. J., Ye, H., Radlinska, A., & Peethamparan, S. (2016). Alkali-activated slag cement concrete. *Concr. Int., 38*(1), 33-38.
42. Wallah, S., & Rangan, B. V. (2006). Low-calcium fly ash-based geopolymer concrete: long-term properties.
43. Wang, K.-t., Du, L.-q., Lv, X.-s., He, Y., & Cui, X.-m. (2017). Preparation of drying powder inorganic polymer cement based on alkali-activated slag technology. *Powder technology, 312*, 204-209.
44. Yang, K.-H., Song, J.-K., Ashour, A. F., & Lee, E.-T. (2008). Properties of cementless mortars activated by sodium silicate. *Construction and Building Materials, 22*(9), 1981-1989.
45. Ye, H., & Radlińska, A. (2016). Shrinkage mechanisms of alkali-activated slag. *Cement and Concrete Research, 88*, 126-135. doi:<https://doi.org/10.1016/j.cemconres.2016.07.001>
46. Yip, C. K., Lukey, G., & van Deventer, J. S. (2005). The coexistence of geopolymeric gel and calcium silicate hydrate at the early stage of alkaline activation. *Cement and Concrete Research, 35*(9), 1688-1697.
47. Zhang, H. Y., Kodur, V., Qi, S. L., Cao, L., & Wu, B. (2014). Development of metakaolin–fly ash based geopolymers for fire resistance applications. *Construction and Building Materials, 55*, 38-45. doi:<https://doi.org/10.1016/j.conbuildmat.2014.01.040>
48. Zhang, M. H., Li, L., & Paramasivam, P. (2005). Shrinkage of high-strength lightweight aggregate concrete exposed to dry environment. *ACI Materials Journal, 102*(2), 86-92.

Figures



(a)



(b)

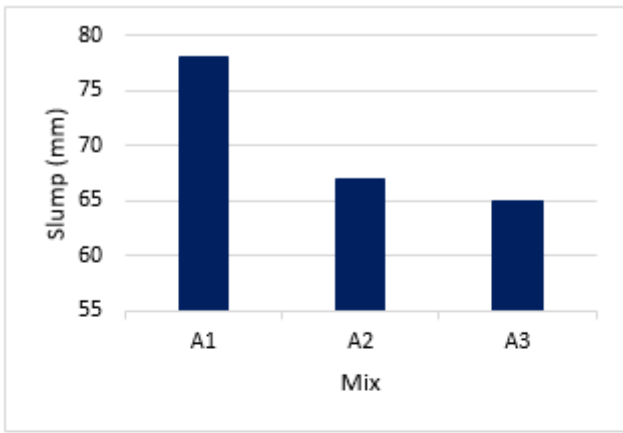
Figure 1

curing condition a) plastic cover curing, b) water curing.

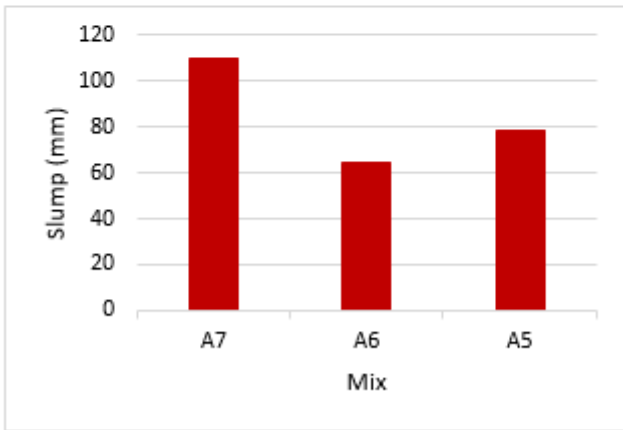


Figure 2

DEMEC gauge.



(a)



(b)

Figure 3

The effect of: a) slag content and sodium metasilicate, b) aggregate combination on slump of OLWAAS concrete.

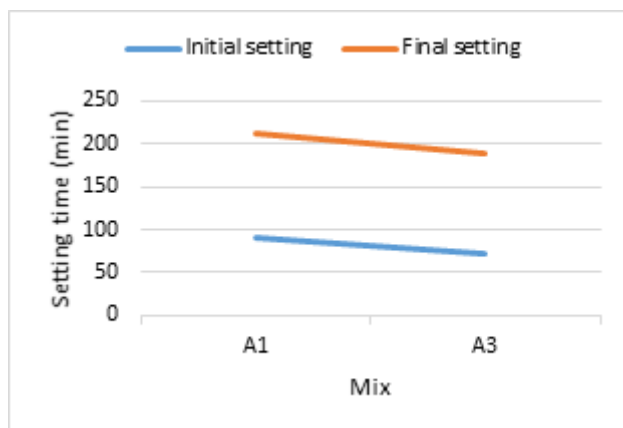


Figure 4

The effect of sodium metasilicate on the setting time.

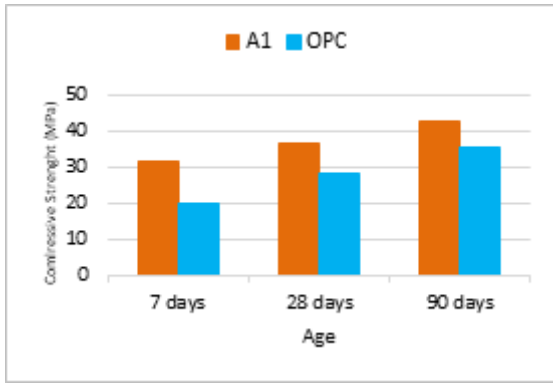
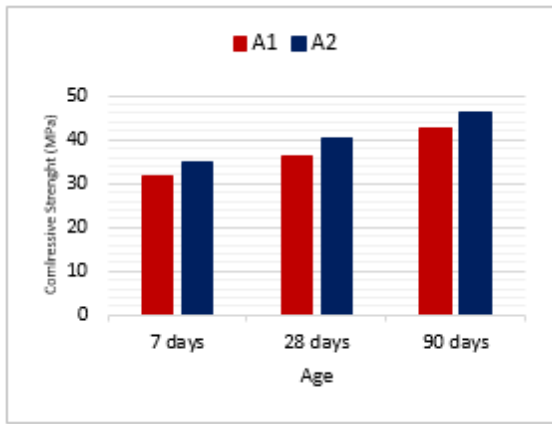
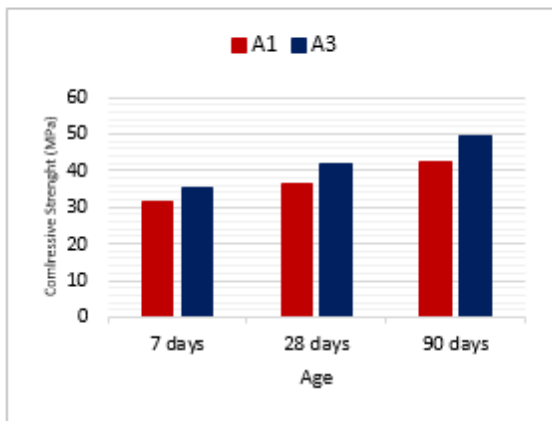


Figure 5

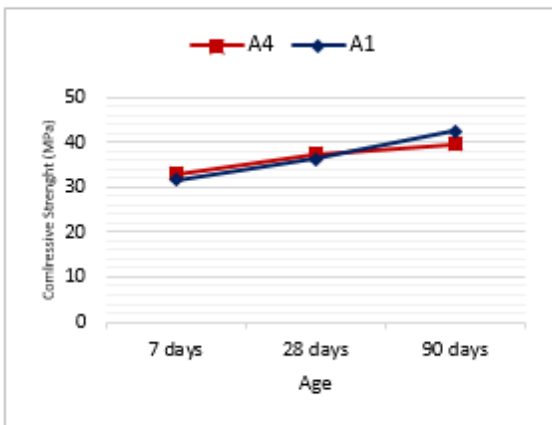
The compressive strength of OLWAAS and LWC concrete.



(a)



(b)



(c)

Figure 6

The compressive strength of OLWAAS concrete based on: a) slag content and sodium metasilicate, c) curing condition.

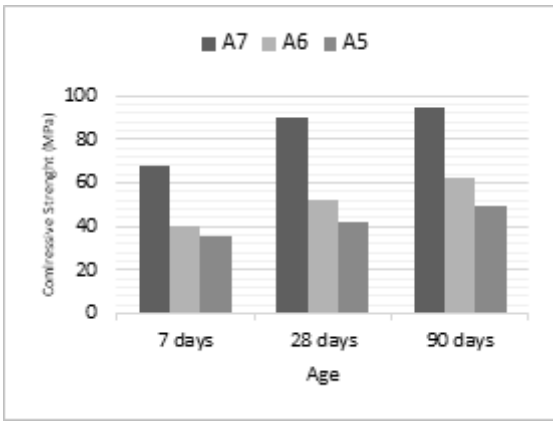


Figure 7

The effect of aggregate combination on the compressive strength.

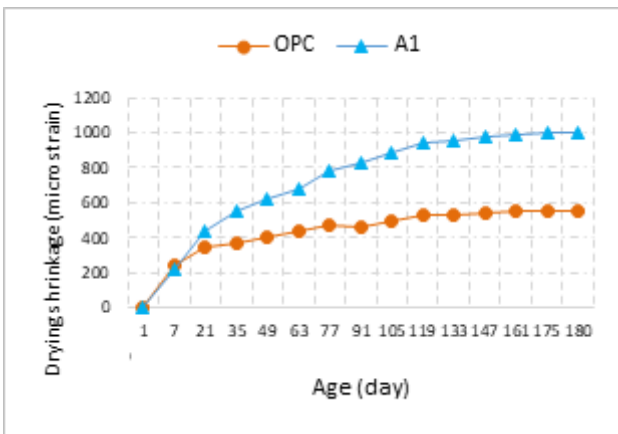
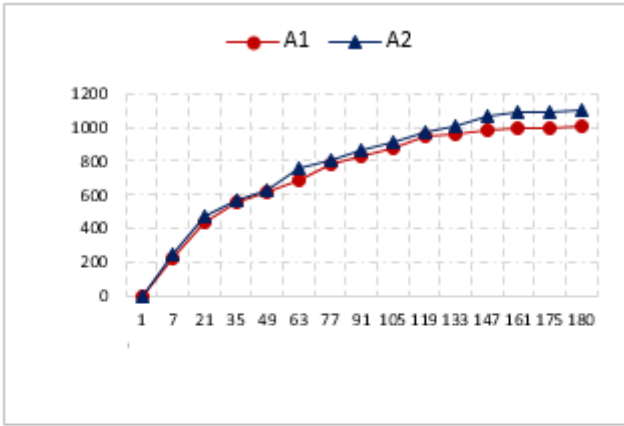
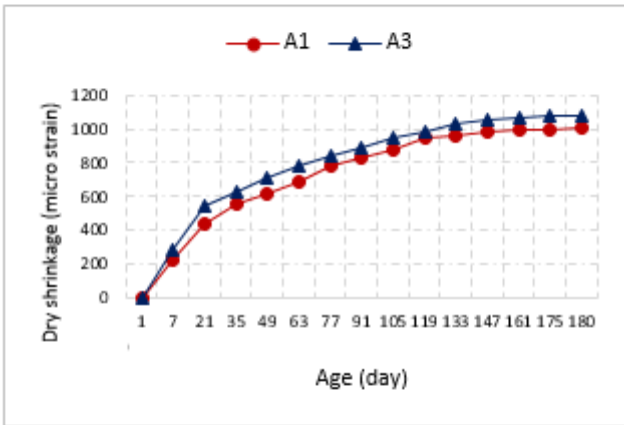


Figure 8

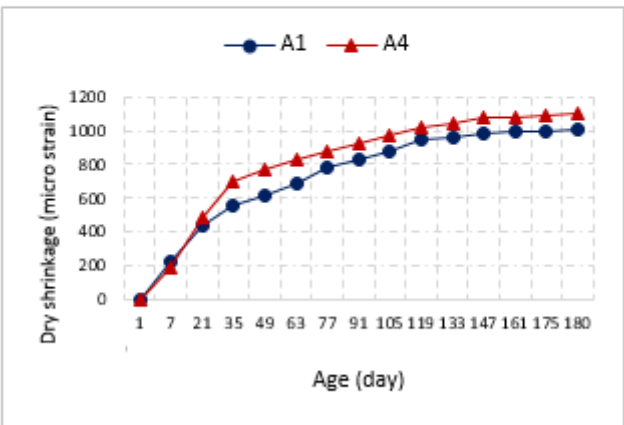
The drying shrinkage of OLWAAS and LWC concrete.



(a)



(b)



(c)

Figure 9

The drying shrinkage of OLWAAS concrete based on: a) slag content, b) sodium metasilicate, c) curing condition.

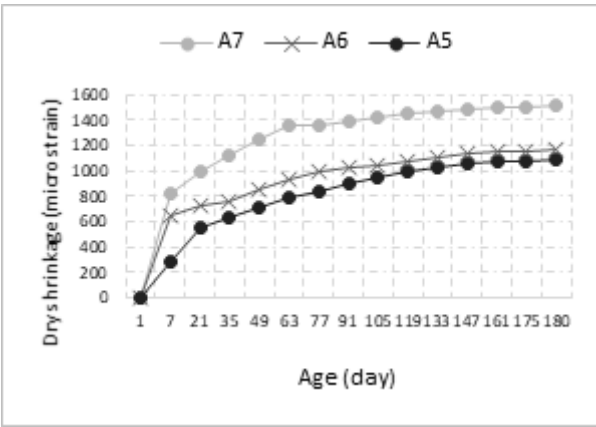
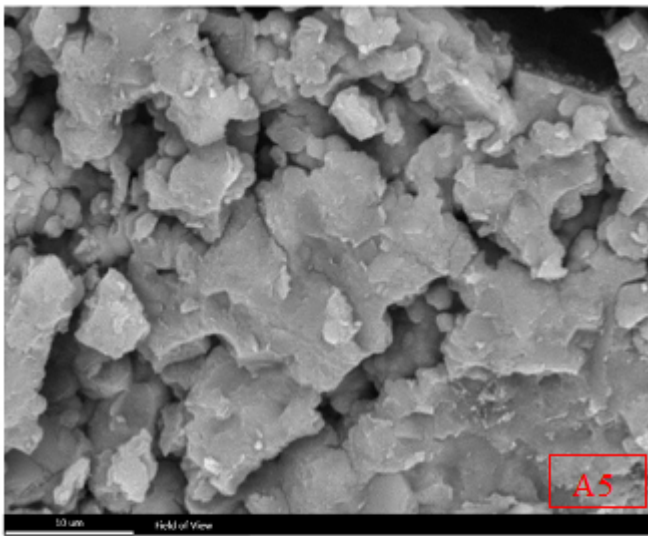
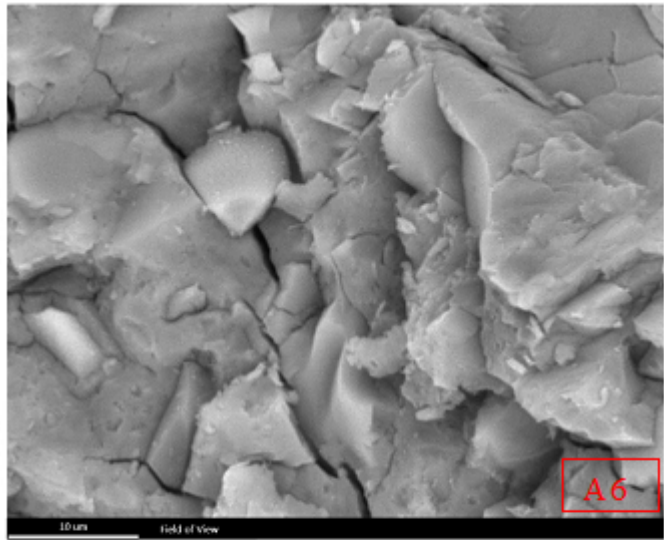


Figure 10

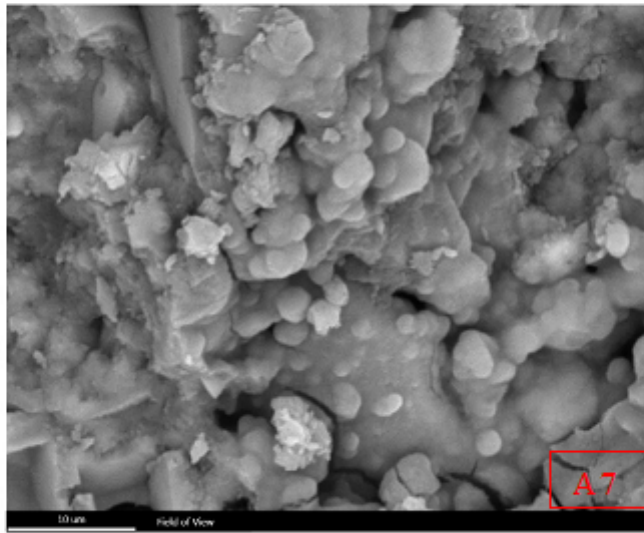
The effect of aggregate combination on the drying shrinkage.



a



b



c

Figure 11

Microstructure of AAS samples: a) A5, b) A6 and c) A7